Economic Geology
Vol. 86, 1991, pp. 983–1001

Hydrothermal Alteration of Mafic Metavolcanic Rocks and Genesis of Fe-Zn-Cu Sulfide Deposits, Stone Hill District, Alabama

YAOLING NIU* AND C. MICHAEL LESHER

Department of Geology, University of Alabama, Tuscaloosa, Alabama 35487-0338

Abstract

Fe-Zn-Cu sulfide mineralization in the Stone Hill district of the northern Alabama Piedmont is hosted by zones of felsic schist and garnet schist within the Ketchepedrakee Amphibolite. The felsic schist is characterized by quartz-pyrrhotite-biotite-muscovite-plagioclase-rutile-sphalerite ± chalcopyrite ± pyrite ± hornblende ± epidote assemblages and the garnet schist is characterized by garnet-hornblende-quartz-biotite-pyrrhotite-chalcopyrite ± sphalerite ± pyrite ± chlorite ± actinolite ± calcite assemblages. Both schists are well banded and highly deformed. The felsic schist locally contains ellipsoidal, polycrystalline aggregates of quartz-feldspar-biotite that superficially resemble sedimentary clasts but clearly formed tectonically by boudinage of felsic bands. The following petrographic and geochemical data and field relationships suggest that both schists are hydrothermally altered basalt (the precursor of the Ketchepedrakee Amphibolite): (1) the felsic and garnet schist units are very localized lenses (<1-km strike length, <50-m thickness); (2) contacts between the felsic schist and the amphibolite are normally gradational and may be transitional through the garnet schist; (3) both schists contain abundant rutile, distributed in the same way as ilmenite in the schists and the amphibolite; (4) the two schists and the amphibolite are uniformly enriched in compatible transition elements such as Sc, Ti, V, Cr, and Co; (5) ratios of incompatible, high field-strength elements such as Y, Zr, Nb, REE, and Hf are virtually identical in the schists and the amphibolite; and (6) the schists and the amphibolite exhibit similar flat chondrite-normalized rare earth element (REE) abundance patterns (with variable Eu anomalies). Textural data indicate that alteration and mineralization of the basaltic protolith predated metamorphism and deformation. The Fe-Zn-Cu sulfide deposits in the Stone Hill district are interpreted to have formed by synvolcanic hydrothermal alteration in an incipiently rifted basin.

Introduction

BASE metal mineralization in the Stone Hill district of the northern Piedmont is hosted by felsic schist and garnet schist within a larger body of amphibolite, near the contact between two thick pelitic metasedimentary sequences. Associated lithologies include tremolite-chlorite rocks and oxide facies iron-formation. Several geologic studies have been done in the area (Pallister and Thoenen, 1948; Espenshade, 1963; Whittington, 1982; Neathery and Hollister, 1984; Stow et al., 1984; Schafer and Coolen, 1986), but poor exposure and a complex metamorphic and deformational history have hampered interpretations of the nature of the host rocks, the genetic history of the ores, and the tectonic setting of the deposits.

The amphibolite which encloses the deposits has been interpreted as a metamorphosed tholeiitic basalt (Whittington, 1982; Stow et al., 1984; Schafer and Coolen, 1986) and the enclosing pelitic metasedimentary rocks have been interpreted as metamorphosed flysch-type sediments (Neathery and Hollister, 1984). The garnet schists and tremolite-chlorite rocks and the oxide facies iron-formations have been interpreted as altered basalts and exhalites, respectively (Whittington, 1982; Schafer and Coolen, 1986). On the basis of the above-lithological associations, their stratigraphic conformability, and the presence of hydrothermally altered rocks and exhalites, the Fe-Zn-Cu deposits in the Stone Hill district have been interpreted by previous investigators as proximal volcanic-associated massive sulfide deposits (cf. Franklin et al., 1981).

There is less unanimity concerning the nature of the mineralized felsic schists and the tectonic setting of the deposits. Whittington (1982) and Stow et al. (1985) interpreted the felsic schists as metasedimentary rocks and concluded that the Stone Hill deposits formed along a spreading margin. Neathery and Hollister (1984) also interpreted the felsic schists as metasedimentary rocks but concluded that all of the deposits in the northern Piedmont formed in a back-arc basin. Although Schafer and Coolen (1986) mentioned the possibility that the felsic schists may have formed by alteration, they interpreted them as rhyolitic metavolcanic-pyroclastic rocks.

The aim of this paper is to report the results of a detailed study to determine the protoliths of the felsic schist and garnet schist and the timing of base metal

* Present address: School of Ocean and Earth Sciences and Technology, University of Hawaii at Manoa, Honolulu, Hawaii 96822.

0361-0128/91/1249/983-19$3.00

mineralization in the Stone Hill district. These data provide important constraints on the environment of deposition of the sulfide deposits and their volcanic and tectonic setting in this part of the southern Appalachians, and they highlight criteria for the recognition of hydrothermal alteration signatures in metamorphosed mafic volcanic rocks.

Geologic Setting

The stratigraphy and lithotectonic framework of the Appalachian Piedmont metamorphic belt in Alabama has been described by Neathery (1975) and Tull (1978). The Stone Hill district occurs in the northern Piedmont in the northeastern salient of the Coosa block along the boundary between the Poe Bridge Mountain and Mad Indian Groups of the Ashland Supergroup. The Stone Hill massive sulfide district (Fig. 1) comprises the Stone Hill copper mine, the Smith copper mine, and three prospects: First Wood's (Micaville prospect of Schafer and Coolen, 1986), Johnson (Section 34 prospect of Schafer and Coolen, 1986), and Chaotic Zone. Diamond drill cores from all areas, except the Smith mine, were studied, including continuous core from recent drilling by Billiton Exploration, Inc. (First Wood's, Johnson, and Chaotic Zone prospect areas) and skeletonized core from earlier drilling by Tennessee Copper Corporation (Stone Hill mine area).

The metamorphic stratigraphy of the Ashland Supergroup in the Stone Hill district, from structurally highest (south) to structurally lowest (north) is summarized as follows (cf. Figs. 1, 2, and 3):

Ashland Supergroup

Mad Indian Group: quartz-muscovite-biotite schist and garnetiferous muscovite-biotite schist; local quartz-muscovite pegmatite; rare amphibolite.

Poe Bridge Mountain Group: Ketchepedrakee Amphibolite (including amphibolite sensu lato and local metagabbro); minor quartz-muscovite-feldspar schist (felsic schist); local garnetiferous schist, tremolite-chlorite schist, and magnetite iron-formation; graphitic quartz-muscovite schist; quartz-muscovite-biotite schist; garnetiferous quartz-muscovite-biotite schist.

This study has concentrated on the Ketchepedrakee Amphibolite country rocks, mineralized zones of felsic schist, and garnet schist which are closely associated with massive sulfide mineralization. It is focused on the First Wood's prospect (Figs. 2 and 3) because it contains all of the major lithologies and appears to be less complexly deformed than other areas in the Stone Hill district.

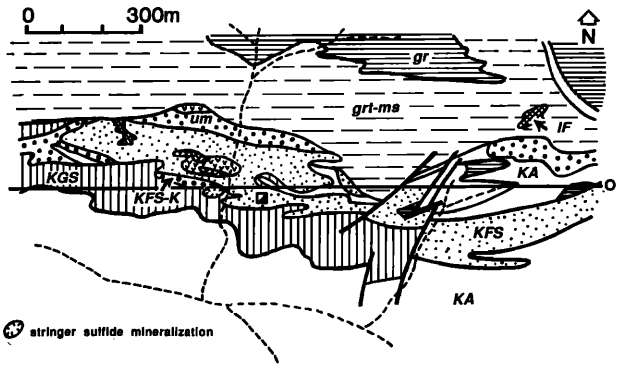

FIG. 2. Geologic map of the First Wood's prospect (modified after Schafer and Coolen, 1986). KA = Ketchepedrakee Amphibolite, KGS = Ketchepedrakee garnet schist, KFS = Ketchepedrakee felsic schist, KFS-K = kyanite-bearing felsic schist, IF = magnetite iron-formation; gr = graphitic schist, grt-ms = garnet-muscovite schist, vvv = "spotty" (retrograde) amphibolite, um = metagabbro, ◪ = main prospect area.

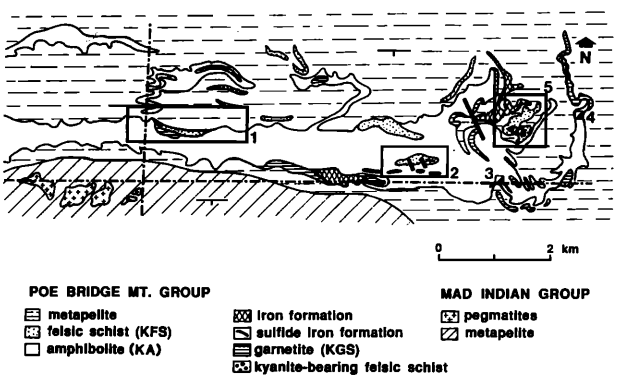

FIG. 1. Generalized geologic map of the Stone Hill district (modified after Schafer and Coolen, 1986). 1 = First Wood's prospect, 2 = Johnson prospect, 3 = Stone Hill mine, 4 = Smith mine, 5 = Chaotic Zone prospect. Rock units as described in text.

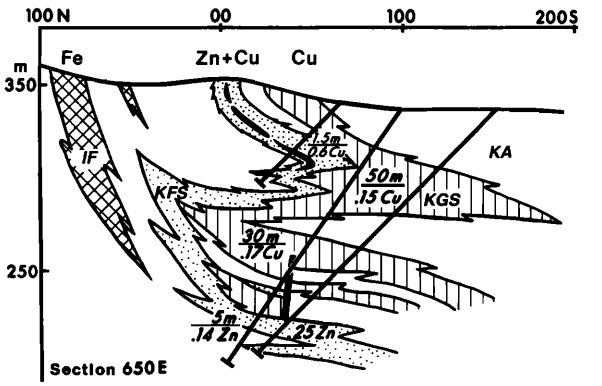

FIG. 3. Cross section of the First Wood's prospect (modified after Schafer and Coolen, 1986) showing metal zonation (facing interpreted to be toward the north). Abbreviations as in Figure 2.

Lithology and Petrography

Field relationships and modal mineralogic analyses (Table 1) show that the rocks in the ore environment at the First Wood's prospect can be subdivided into five lithologies: Ketchepedrakee Amphibolite, Ketchepedrakee garnet schist, and three varieties of mineralized Ketchepedrakee felsic schist: hornblende rich, biotite rich, and muscovite rich. The detailed petrography of these lithologies is given in Niu (1988) and the major characteristics which constrain the nature of the protolith of these lithologies are summarized as follows.

Petrography

Ketchepedrakee Amphibolite: The outcrop belt of Ketchepedrakee Amphibolite (Figs. 1 and 2) ranges from less than 100 to over 1,000 m in width. Contacts between the amphibolite and the surrounding metasedimentary rocks (Poe Bridge Mountain Group) are sharp and appear conformable (Stow et al., 1984). In the Stone Hill district (Fig. 1), the amphibolite occurs on the northwest limb of an overturned anticline within the Poe Bridge Mountain Group (Schafer and Coolen, 1986). The amphibolite is a fine- to medium-grained, schistose mafic rock characterized by the assemblage hornblende-quartz-oligoclase-ilmenite-calcite-biotite-epidote (Fig. 4A). Most importantly, it is characterized by abundant ilmenite which occurs as elongate grains or aggregates, distributed along the principal foliation and concentrated in microcrenulation fold hinges. No sulfide phases have been recognized in it.

Ketchepedrakee garnet schist: The garnet schist occurs as isolated lenses within amphibolite, closely associated with mineralized felsic schist (described below) (Fig. 1). The garnet schist is characterized by the assemblage garnet-hornblende-quartz-biotite-pyrrhotite-chalcopyrite-sphalerite-pyrite-chlorite-actinolite-calcite (Fig. 4B). The garnet is usually coarse grained (up to 10–15 mm), fracture filled by quartz, calcite, and sulfides, and replaced by chlorite, actinolite, quartz, and calcite. Abundant rutile occurs mainly as fine-grained inclusions in both garnet (Fig. 4B) and biotite, defining a prepeak metamorphic foliation. Some rocks are relatively massive, but most are strongly deformed into garnet schist, and in some rocks garnet is so sheared that quartz inclusions are deformed into discrete bands.

Ketchepedrakee felsic schist: The felsic schist occurs as lenses within the Ketchepedrakee Amphibolite; major units are exposed at the First Wood's (Figs. 2 and 3), Johnson, and Chaotic Zone prospects, and at the Stone Hill mine (Fig. 1). They are generally less than 0.2 km^2 in outcrop area (Figs. 1–3), less than 1 km in strike length, and less than 50 m in downhole thickness (Fig. 3). Lenses and pods of amphibolite are very common within the felsic schist; contacts with amphibolite are gradational over a distance of several decimeters. The felsic schist is strongly deformed, typically banded and folded. Fe-Cu-Zn sulfide mineralization increases with increasing grain size, the proportion of felsic bands, especially in fold hinges, and the proportion of quartz-carbonate veins and accompanying alteration. The felsic schist may be subdivided into three groups based on modal mineralogy (Table 1; Niu, 1988): hornblende rich, biotite rich, and muscovite rich. The hornblende-rich felsic schist is mineralogically gradational between the amphibolite and the biotite-rich felsic schist, and occurs spatially transitional between them and as layers or pods within biotite-rich felsic schist. The hornblende-rich felsic schist is a generally coarse-grained, recrystallized, mineralogically complex rock characterized by variable amounts of hornblende (10–60%), abundant calcite, lesser amounts of actinolite, epidote, and albitic plagioclase, and minor garnet, biotite, chlorite, rutile, sphene, ilmenite, and sulfides (Fig. 4C). Biotite, hornblende, ilmenite-rutile, and sulfides define the principal foliation. Adjacent to carbonate veins or veinlets, prograde metamorphic phases may be completely replaced by actinolite, quartz, epidote, clinozoisite, albite, secondary garnet and secondary biotite, quartz, chlorite, and calcite. With decreasing hornblende content, ilmenite decreases in abundance and rutile-sphene increases in abundance. With increasing biotite and sulfide content, the hornblende-rich felsic schist grades into biotite-rich felsic schist. With increasing garnet content, the hornblende-rich felsic schist grades into the garnet schist.

The biotite- and muscovite-rich felsic schists are gradational and are composed of variable amounts of quartz, plagioclase, potassium feldspar, biotite (or phlogopite), muscovite, garnet, hornblende, staurolite, calcite, clinozoisite, epidote, and apatite (Fig. 4D and E). The muscovite-rich felsic schist commonly contains abundant kyanite which is retrograded to sericite. The biotite- and muscovite-rich felsic schists both contain abundant sulfides, predominantly pyrrhotite with minor sphalerite, chalcopyrite, and pyrite. Fine-grained (<0.5 mm) rutile is ubiquitous in disseminated layers, as isolated disseminated grains, and as inclusions in biotite, staurolite, and garnet (Fig. 4F). Quartz, feldspar, rutile, and sulfides define the principal foliation in these rocks (Fig. 4D–F). Biotite-phlogopite, garnet, and minor hornblende exhibit simple contact textures, but all are variably replaced by chlorite, calcite, and sulfides due to retrograde alteration and remobilization of carbonates, silica, and sulfides.

The felsic schist at the Stone Hill mine is similar to that at the First Wood's prospect. It is characterized by abundant quartz, plagioclase, potassium feldspar, biotite, muscovite, and rutile, plus lesser garnet,

TABLE 1. Modal Mineralogy of Principal Lithologies at the First Wood's Prospect, Stone Hill District, Alabama (modal vol %; data from Niu, 1988)

	KA				KGS				KFS-H				KFS-B				KFS-M			
	Mean	Range	1σ	n	Mean	Range	1σ	n	Mean	Range	1σ	n	Mean	Range	1σ	n	Mean	Range	1σ	n
Actinolite					4.5	2–8	2.7	4	2.1	0–12	4.4	8	2.9	0–20	7.6	7				
Apatite									0.6	0–1	0.5	8	0.4	0–2	0.8	7	0.3	0–1	0.6	3
Biotite	1.1	0-3	1.1	9	3.0	0–6	2.5	4	21.0	7–40	9.7	8	18.9	10–30	6.4	7	3.7	1–7	3.1	3
Calcite	2.1	1-4	1.1	9	4.3	2–5	1.5	4	7.5	2–20	6.4	8	1.0	0–5	1.8	7				
Chlorite	0.8	0-2	0.7	9	6.5	3–11	3.4	4	1.1	0–2	0.6	8	0.1	0–1	0.4	7				
Epidote	2.1	1-8	2.3	9	1.0	1–1	0.0	4	2.9	1–5	1.8	8	1.5	1–4	1.1	7	0.7	0–1	0.6	3
Gahnite													0.3	0–2	0.8	7				
Garnet					50.5	44–67	11.0	4	2.9	0–10	4.5	8	2.9	0–8	2.9	7	1.7	0–5	2.9	3
Hornblende	62.4	60-70	4.0	9	9.0	0–19	9.4	4	20.3	5–48	15.6	8	1.0	0–5	1.9	7				
Ilmenite	4.4	4-5	0.5	9					0.3	0–2	0.7	8								
Kyanite																	1.0	0–3	1.7	3
Muscovite													4.0	1–10	4.2	7	46.7	40–50	5.8	3
Orthoclase									0.8	0–3	1.0	8	2.7	0–5	2.4	7	2.3	1–5	2.3	3
Plagioclase	13.3	10-17	3.0	9	4.5	2–8	3.0	4	14.5	5–21	4.9	8	16.9	10–20	3.9	7	6.0	5–8	1.7	3
Quartz	13.7	5-20	4.3	9	6.5	5–10	2.4	4	17.1	13–20	3.0	8	31.3	18–48	9.9	7	15.0	5–20	8.7	3
Rutile					4.3	3–5	1.0	4	2.4	1–4	0.9	8	2.9	2–4	0.9	7	4.3	4–5	0.6	3
Sericite					0.5	0–1	0.6	4	0.1	0–1	0.4	8					6.7	0–20	11.6	3
Sphene									0.6	0–2	0.9	8								
Staurolite													4.9	0–19	8.38	7				
Sulfide					5.5	5–7	1.0	4	5.8	2–15	4.8	8	8.6	3–20	6.40	7	11.7	10–15	2.9	3
Total	99.9				100.1				100.0				100.1				100.0			

Abbreviations: KA = Ketchepedrakee Amphibolite, KGS = Ketchepedrakee garnet schist, KFS–H = hornblende–rich Ketchepedrakee felsic schist, KFS–B = biotite–rich Ketchepedrakee felsic schist, KFS–M = muscovite–rich Ketchepedrakee felsic schist, *n* = number of samples examined

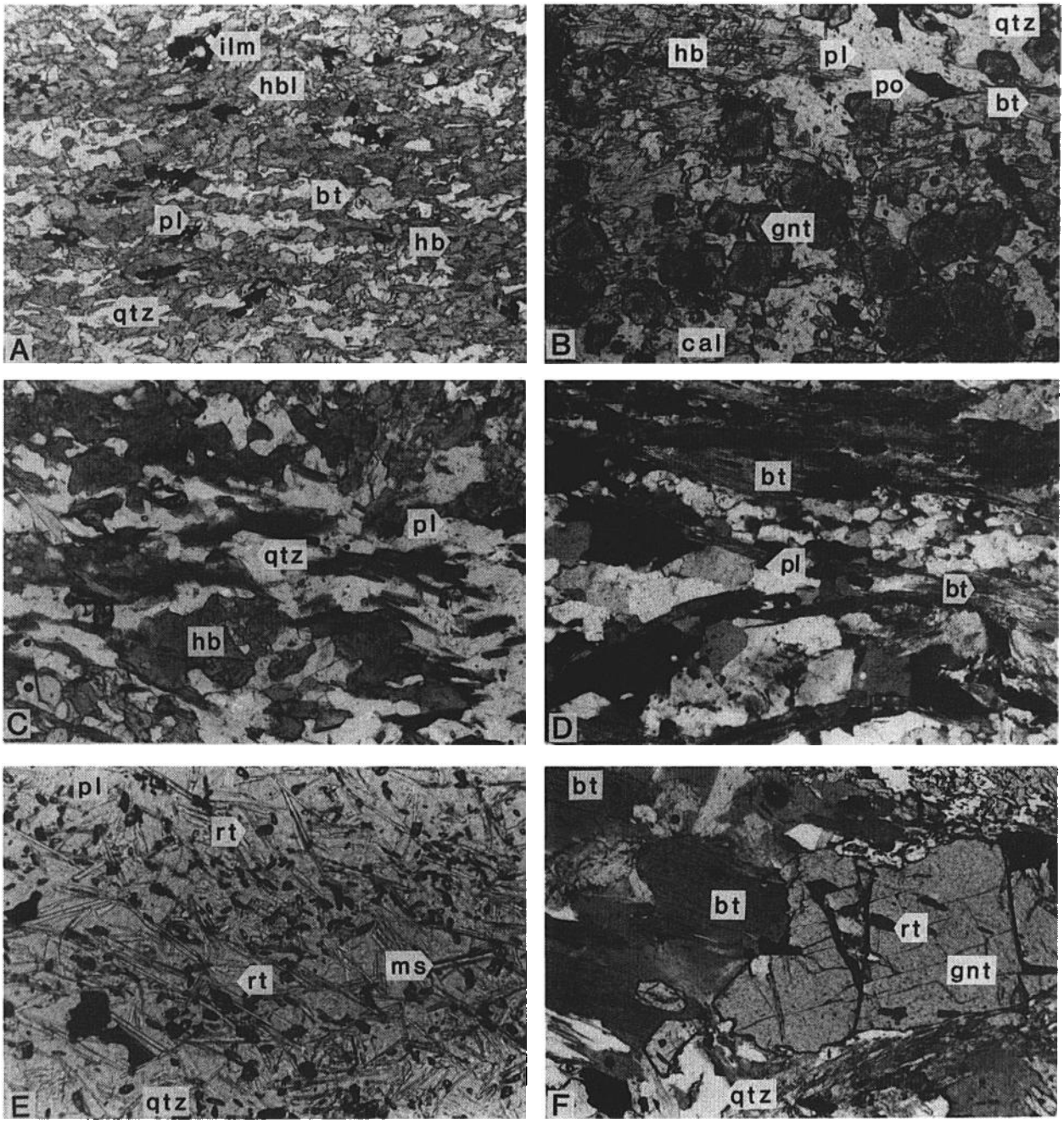

FIG. 4. Representative photomicrographs of unmineralized Ketchepedrakee Amphibolite, garnet schist, and felsic schist at the First Wood's prospect, highlighting textures, mineralogy, and abundance of Ti phases. A. Ketchepedrakee Amphibolite. B. Ketchepedrakee garnet schist. C. Hornblende-rich Ketchepedrakee felsic schist. D. Biotite-rich Ketchepedrakee felsic schist. E. Muscovite-rich Ketchepedrakee felsic schist. F. Transitional felsic schist–biotite-rich felsic schist. Transmitted, plane-polarized light except cross-polarized light for E and F; 2.7 mm field of view. Abbreviations: bt = biotite, cal = calcite, chl = chlorite, grt = garnet, hbl = hornblende, ilm = ilmenite, ms = muscovite, pl = plagioclase, po = pyrrhotite, qtz = quartz, rt = rutile.

hornblende, epidote, clinozoisite, carbonates, and sulfides (Fig. 5A). Rutile is distributed identically to that in the First Wood's prospect, occurring as fine euhedral grains or as layers and microbands parallel to the schistosity and/or folded together with other elements of the rock fabric (Fig. 5B). The principal

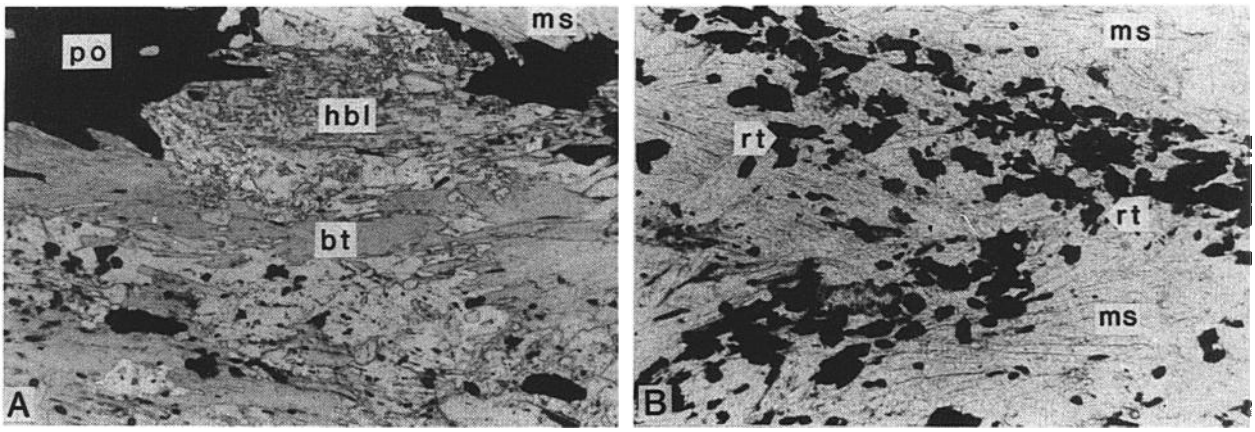

FIG. 5. Representative photomicrographs of mineralized felsic schist at the Stone Hill mine. A. Biotite-rich Ketchepedrakee felsic schist. B. Muscovite-rich Ketchepedrakee felsic schist. Note abundant fine-grained rutile defining S_1 foliation. Transmitted, plane-polarized light; 2.7 mm field of view; abbreviations as in Figure 4.

difference between the felsic schist at the two localities is that at the Stone Hill mine it contains slightly more quartz and potassium feldspar, less carbonate, and exhibits less schistose, more recrystallized, equigranular textures.

Deformation and metamorphism

All lithologies in the Stone Hill district have undergone polyphase penetrative deformation and amphibolite facies regional metamorphism (Neathery, 1967; Tull, 1978; Schafer and Coolen, 1986; Niu, 1988). Summarized in Table 2 are these deformational events which provide constraints on the relative timing of alteration and mineralization. Some important textures regarding the nature of the Ketchepedrakee felsic schist are briefly discussed below.

Some felsic schist samples exhibit pseudoclastic textures (Fig. 6A and B). The clasts are irregular, randomly distributed, rounded, and/or ellipsoidal aggregates of mono- and polycrystalline quartz, quartz-feldspar, and quartz-feldspar-biotite within a fine-grained, sheared quartz-feldspar-mica-sulfide-chlorite matrix. They are variable in size (0.2–4 mm) and the grains within individual aggregates exhibit sutured boundaries or equilibrium 120° dihedral angles. The aggregates superficially resemble detrital sedimentary grains or volcanic lapilli, but systematic microscopic examination indicates that they are neither sedimen-

TABLE 2. Structural and Metamorphic History of the Northern Alabama Piedmont (Tull, 1878), Stone Hill District (Schaffer and Coolen, 1986), and First Wood's Prospect (Niu, 1988)

Northern Alabama Piedmont	Stone Hill district	First Wood's prospect
D_1 S_1 foliation	D_1 S_1 foliation	D_1 S_1 foliation
F_1 mesoscopic flow folds	F_1 macroscopic folds	F_1 mesoscopic flow folds?
L_1 mineral lineation	M_p prograde metamorphism	L_1 mineral lineation
M_p prograde metamorphism		M_p prograde metamorphism
D_2 S_2 mesoscopic foliation		
F_2 crenulation folds		
M_r retrograde metamorphism		
D_3 F_3 mesoscopic-macroscopic folds	D_2 F_2 open, asymmetric, macroscopic folds	D_2 F_2 asymmetric, mesoscopic folds
S_3 crenulation cleavage	S_2 crenulation cleavage	S_2 crenulation cleavage
	L_2 intersection lineation	L_2 intersection lineation
		M_p continuing prograde metamorphism
D_4 Hollins Line fault system		D_3 S_3 fractures filled by quartz-carbonate veins
		M_r retrograde alteration
D_5 Megascopic-mesoscopic folds	D_3 F_3 cross folds	D_4 S_4 shearing fabric
		F_4 microscopic folds
		M_r retrograde alteration
D_6 Goodwater-Enitachopco fault system		

D = deformation, F = fold, L = lineation, M = metamorphism, S = foliation

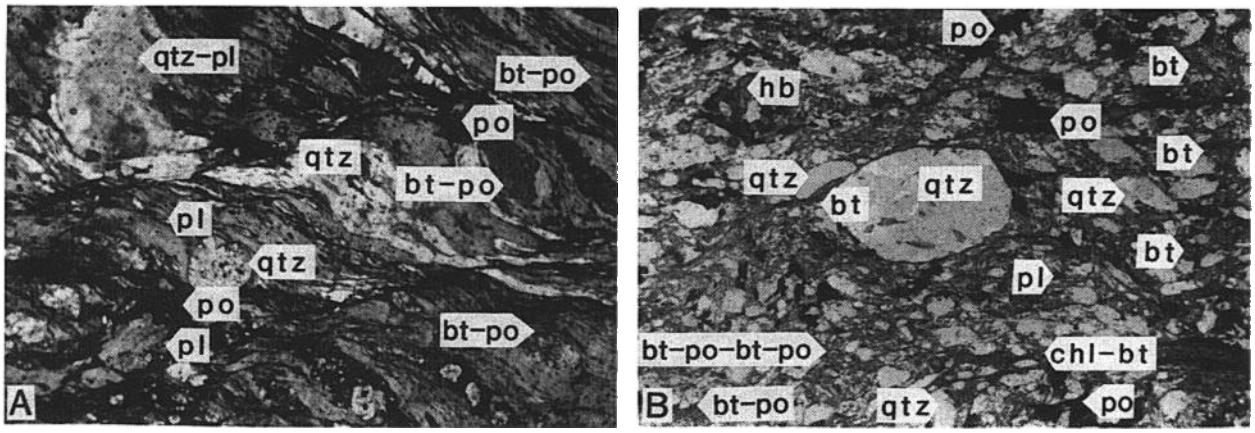

FIG. 6. Photomicrographs illustrating development of pseudoclastic textures in the felsic schist. (a). Microshears separating felsic bands. (b). Polycrystalline aggregates concentrated at intersection of two microshears and rounded quartz-feldspar aggregates. Transmitted, plane-polarized light; 2.7 mm field of view; abbreviations as in Figure 4.

tary clasts nor volcanic lapilli but of tectonic origin. They have been generated through differential shearing of the metamorphosed and recrystallized rocks in response to D_4 deformation (see Table 2). The evidence for such an interpretation includes:

1. The aggregates are confined to D_4 deformation shear zones where felsic and mafic assemblages have been separated into discrete bands. Hornblende grains that are similarly confined within sheared bands are also rounded and garnet grains are rotated.
2. The aggregates are elongate parallel to S_4 foliation, markedly oblique to S_1 and S_2 foliations.
3. The evolution of such textures is progressively preserved in thin sections of spatially adjacent samples (within a few meters) as: (i) initiation of D_4 deformation shearing along mica-sulfide layers (Fig. 6a), (ii) segregation of felsic bands, (iii) boudinage of felsic bands, (iv) deformation of boudins into lenses, and (iv) rotation of lenses into subangular to rounded, ellipsoidal grains (Fig. 6b).

Retrograde metamorphism is limited to the mineralized felsic and garnet schists and is characterized by local silicification, carbonation, and/or remobilization of carbonates in the form of carbonate-quartz veins and veinlets. Silicification involves addition of quartz and replacement of hornblende and plagioclase by albite, tremolite, epidote, Mg chlorite, secondary garnet, and rutile. Secondary garnet is characterized by abundant euhedral epidote inclusions. Carbonation-remobilization of carbonates involves (i) recrystallization of calcite as isolated grains and introduction in veins or veinlets, (ii) enrichment of sulfides along and toward carbonate-quartz veins and veinlets, (iii) replacement of hornblende and plagioclase by coarse-grained epidote, clinozoisite, albite, biotite, and chlorite, and (iv) replacement of rutile by sphene adjacent to carbonate-quartz veinlets or in carbonate-rich domains.

Sulfide mineralization

Fe-Cu-Zn mineralization in the Stone Hill district is characterized by abundant hexagonal pyrrhotite, minor chalcopyrite, sphalerite, and pyrite, plus trace amounts of arsenopyrite and gahnite. Chalcopyrite is enriched in garnet schists, sphalerite in felsic schists. The ores occur primarily as stratiform massive (>60% sulfides), semimassive (20–60% sulfides), and disseminated (<20% sulfides) sulfides within felsic schists, and as strata-bound disseminated mineralization within garnet schists. Schafer and Coolen (1986) report that ore grades at the Stone Hill mine range from 0.05 to 3.0 percent Cu and from 0.85 to 1.8 percent Zn, with minor Pb, Ni, and Co and trace amounts of Au and Ag; thin massive pyrrhotite layers at the First Wood's prospect contain up to 7 percent Zn and up to 1 percent Cu.

Sulfides occur as elongate aggregates subparallel to S_1 foliation and have been extensively redeformed and remobilized during all four documented stages of deformation. This indicates that the mineralization predates peak regional metamorphism and deformation. The sulfides appear to have responded to deformation with different degrees of ductility in the order: chalcopyrite > sphalerite > pyrrhotite > pyrite. Sulfides are redistributed into the noses of F_2 folds (Schafer and Coolen, 1986) and are concentrated along carbonate-quartz veins or veinlets. Relatively ductile sulfides, such as sphalerite, chalcopyrite, and pyrrhotite, have been introduced along the interstices of garnet, plagioclase, and quartz, along cleavage planes in hornblende and biotite, and into sheared voids of silicate minerals. In contrast, relatively brittle

sulfides such as pyrite are strongly fractured. Some pyrite occurs as unfractured, anhedral grains which contain concentrically distributed pores. Similar textures have been described by Carpenter (1974) elsewhere in the southern Appalachians, possibly representing transformation of pyrrhotite into pyrite during retrograde metamorphism.

Geochemistry

It has been successfully demonstrated that the mobilities of various elements during hydrothermal alteration and metamorphism can be evaluated and that the nature and geochemical signatures of such processes can thereby be determined (Holland and Winchester, 1983; Rösler and Beuge, 1983; Campbell et al., 1984; Lesher et al., 1986b). Mobile elements provide information concerning the alteration processes, whereas immobile elements retain the geochemical signature of the protolith. Thus, the differential mobility of various elements during hydrothermal alteration and regional metamorphism can be used to infer the protoliths of the lithologies and to deduce their hydrothermal and metamorphic history.

The mobility of elements during various hydrothermal processes can be predicted in terms of their geochemical characteristics. Major elements such as Si, Al, Fe, Mg, Mn, Ca, Na, and K are generally mobile during hydrothermal alteration because they are housed in rock-forming minerals that are dissolved or precipitated in the acid, reduced, saline hydrothermal fluids. These same elements are normally less mobile during metamorphism because metamorphic fluids in pelitic schists and gneisses are generally only slightly acidic, near-neutral, and H_2O-CO_2 rich. Large ion lithophile elements such as Cs, Rb, Ba, and Sr are mobile in both hydrothermal and metamorphic fluids because they are housed primarily in feldspars, which alter readily, or in micas, which are common alteration products. They also have low field strengths (charge/ionic radius) and are therefore easily complexed and transported in fluids. First-period transition metals such as Sc, Ti, V, Cr, Mn, Fe, Co, Ni, Cu, and Zn are hosted by a variety of silicates, oxides, and sulfides. Their mobility is dependent to a large degree upon quantum mechanics (Brimhall and Crerar, 1987); elements with high ligand field stabilization energies (e.g., V, Cr^{+3}, and Ni in octahedral coordination, Ti and Co in tetrahedral coordination) are less mobile than those with low ligand field stabilization energies (e.g., Sc, Mn, Fe, and Zn in octahedral coordination, Cr, Mn, Cu, and Zn in tetrahedral coordination). They may remain relatively immobile during metamorphism as one phase is replaced by another, but all are mobile to varying degrees during spilitization and chloritization (e.g., Lesher et al., 1986b). High field strength elements such as Y, Zr, Nb, and Hf, plus the rare earth elements (REE: La-Lu), are least mobile because they are housed primarily in accessory phases, which resist alteration, and because they have high field strengths and are therefore not as easily complexed and transported in hydrothermal fluids. (Exceptions are Ce which may be quadrivalent and mobilized under oxidizing conditions, and Eu which may be divalent and mobilized under reducing conditions.) The trivalent REE are particularly useful petrogenetic indicators because they systematically decrease in ionic radius with increasing atomic number and therefore exhibit very systematic signatures that are related to site size in the host mineral(s).

Together, the relative mobility of the elements within these four groups may be used to infer the petrogenetic affinity of the igneous protolith, and the nature and composition of the hydrothermal metamorphic fluids. Because different elements are concentrated in different phases (e.g., light REE in apatite and monazite, heavy REE in zircon and sphene, Eu in feldspar, Zr and Hf in zircon) which have different stabilities, element mobility resulting from mineral breakdown should result in changes in elemental ratios. Changes in the absolute abundances of elements during alteration is not necessarily evidence of elemental mobility, because the absolute abundances of elements may be modified by concentration-dilution during enrichment-depletion of other elements or by changes in rock volume (Gresens, 1967; Campbell et al., 1984).

Geochemical analysis and results

Thirty-one samples of the five major lithologies from the First Wood's prospect (9 Ketchepedrakee Amphibolite, 4 Ketchepedrakee garnet schist, 8 hornblende-rich Ketchepedrakee felsic schist, 7 biotite-rich Ketchepedrakee felsic schist, and 3 muscovite-rich Ketchepedrakee felsic schist) and four samples of Ketchepedrakee felsic schist from the Stone Hill mine have been analyzed for major, minor, and trace elements. Analytical instrumentation, methods, and uncertainties are described in detail by Niu (1988). Major (Si, Ti, Al, Fe, Mg, Ca, and Na), minor (Mn and P), and selected trace elements (Ni, Cu, Zn, Rb, Sr, Y, Zr, and Nb) were determined by wavelength dispersive XRF spectrometry at the University of Alabama. Additional trace elements (Ba, Sc, V, Cr, Co, La, Ce, Sm, Eu, Dy, Yb, Lu, and Hf) were determined by INAA at the Oak Ridge National Laboratory and the University of Toronto. Sulfur was determined by inductive combustion using a Leco SC-132 automatic titrator at the University of Alabama.

The mean whole-rock geochemical compositions, ranges, and standard deviations of the five principal rock types from the First Wood's prospect and felsic schist from the Stone Hill mine are given in Table 3.

Exclusive of sulfides, the amphibolite and garnet schist have whole-rock major element compositions (in terms of CIPW norms: Niu, 1988) typical of mafic igneous rocks, whereas those of felsic schist vary from mafic (hornblende rich) through intermediate (biotite rich) to felsic (muscovite rich). Relative to most mafic igneous rocks (Carmichael et al., 1972), the amphibolite is slightly enriched in Na and K; the garnet schist is enriched in divalent first-period transition metals (Mn, Fe, Co, Ni, Cu, and Zn) and V, and depleted in large ion lithophile elements; and the felsic schist is enriched in Rb, K, Ba, Mn, and Zn (and to a lesser extent Fe and Cu), and depleted in Sr and Ca (and to a lesser extent Mg and Ni).

Despite significant differences in modal mineralogy (Table 1) and major element chemistry, the trace element geochemical compositions of the five rock types (Table 3) are similar. All are characterized by relatively flat chondrite-normalized REE abundance patterns, with variable Eu anomalies (Fig. 7A–D). The ranges of abundances of REE elements between groups are not significantly different, and their interelement ratios are relatively constant (Table 3). Immobile elements such as Y, Zr, Nb, Hf, Ti, and P exhibit relatively constant ratios in all five rock types (Table 3) and cluster tightly in conventional geochemical discrimination diagrams (Niu, 1988), falling within the fields of subalkalic basalt from ocean-floor or within-plate settings (depending on the classification on which the diagram is based). All five rock types also exhibit relatively consistent and high abundances of compatible elements such as Sc, Ti, V, Cr, and Co (Fig. 8A–E). Ni is more chalcophile and exhibits more dispersion, possibly owing to remobilization in the more sulfur-rich rocks (Fig. 8F). Major and light ion lithophile elements scatter in all rock types (Fig. 9A–F). The excellent correlation between K and Rb (Fig. 9E) reflects their similar geochemical characteristics; Sr and Ca are also correlated but exhibit somewhat greater dispersion (Fig. 9F), reflecting differential mobility during carbonation (discussed below).

The major element geochemical composition of felsic schist from the Stone Hill mine is not significantly different from that of the schist at the First Wood's prospect (Table 3). The felsic schist at Stone Hill is similar to muscovite-rich felsic schist at the First Wood's prospect, albeit somewhat richer in SiO_2, but the range of TiO_2 contents is similar. The trace element concentrations, however, are significantly different. Whereas the REE and high field strength element abundances and interelement ratios of the First Wood's felsic schist are relatively constant, those at the Stone Hill mine are considerably more variable. Some Stone Hill samples are enriched in light REE relative to samples from the First Wood's, whereas others are depleted in light REE (Fig. 7); high field strength elements (Ti, Y, Zr, Nb) are similarly variable. Schafer and Coolen (1986) reported relatively low Zr contents in felsic schist from the First Wood's prospect (107–138 ppm: 2 samples), but higher, more variable Zr contents in felsic schist from the Chaotic Zone and Johnson prospects (355–934 ppm: 3 samples).

Discussion

Nature of the Ketchepedrakee Amphibolite

The Ketchepedrakee Amphibolite appears to exhibit geochemical affinities with midocean ridge basalts (Whittington, 1982; Stow et al., 1984; Schafer and Coolen, 1986), and most workers agree on a tholeiitic basaltic protolith for that lithology. The trace element geochemical data in this study (Table 3) are certainly compatible with that interpretation. In conventional basaltic discrimination diagrams, Ketchepedrakee Amphibolite data are clustered in the fields of subalkalic basalt from ocean-floor or within-plate environments. The clustering of high field strength elements indicates that they have retained constant interelement ratios and have remained relatively immobile during alteration and metamorphism (Niu, 1988).

The Y/Nb ratio is an important discriminant for evaluating the alkalinity of basic igneous rocks (Pearce and Cann, 1973): $Y/Nb < 1$ for alkalic basalts, $1 < Y/Nb < 2$ for transitional basalts, and $Y/Nb > 2$ for tholeiitic basalts. The Y/Nb ratios of the Ketchepedrakee Amphibolite at the First Wood's prospect (Table 2) range between 3.1 and 5.0 and may therefore be classified as tholeiitic (Niu, 1988). This suggests that the high Na and K contents of the Ketchepedrakee Amphibolite, which are higher than expected for tholeiitic basalts, are probably attributable to alteration, consistent with the scatter of these and other mobile elements on geochemical diagrams (Figs. 10A–F).

Nature of the mineralized Ketchepedrakee felsic schist

Whittington (1982), Stow et al. (1985), and Neathery and Hollister (1984) interpreted the Ketchepedrakee felsic schist as metamorphosed sedimentary clastic rock based on major element geochemistry and the sediment-dominated nature of the rock sequence in the area. In contrast, Schafer and Coolen (1986) interpreted it as metamorphosed rhyolite or felsic pyroclastic rock based on trace element geochemistry, specifically high Zr contents, although they did mention the possibility of an origin by alteration of the precursor of the amphibolite.

This study suggests that Ketchepedrakee garnet schist and felsic schist (including the hornblende-, biotite-, and muscovite-rich felsic schists) at the First Wood's prospect are hydrothermally altered equivalents of the amphibolite and that the previous inter-

TABLE 3. Whole-Rock Geochemistry of Principal Lithologies at the First Wood's Prospect and Stone Hill Mine, Stone Hill District, Alabama (data from Niu, 1988)

	KA					KGS					KFS-H				
	Mean	Min	Max	1σ	n	Mean	Min	Max	1σ	n	Mean	Min	Max	1σ	n
SiO_2	48.2	46.6	50.8	1.40	9	47.6	45.4	50.0	2.08	4	48.5	45.6	55.2	3.09	8
TiO_2	1.80	1.19	2.26	0.32	9	1.71	1.55	1.83	0.12	4	1.85	1.60	2.28	0.25	8
Al_2O_3	15.8	14.5	18.7	1.28	9	15.8	14.6	16.5	0.83	4	15.3	11.9	17.2	1.60	8
FeOt	11.9	9.86	14.4	1.41	9	21.3	18.7	23.8	2.25	4	13.0	10.5	15.3	1.97	8
MnO	0.19	0.09	0.26	0.06	9	0.33	0.19	0.66	0.22	4	0.31	0.15	0.55	0.17	8
MgO	6.70	5.02	8.16	1.20	9	5.26	4.57	6.19	0.71	4	4.49	2.42	6.53	1.41	8
CaO	9.77	7.95	12.6	1.65	9	3.48	2.72	4.27	0.82	4	7.17	2.03	10.2	3.15	8
Na_2O	3.44	2.76	4.68	0.65	9	2.20	1.39	2.97	0.67	4	4.01	2.38	5.81	1.12	8
K_2O	0.53	0.07	1.46	0.45	9	0.28	0.11	0.46	0.16	4	1.39	0.12	2.14	0.65	8
P_2O_5	0.24	0.13	0.32	0.08	9	0.20	0.17	0.24	0.03	4	0.21	0.01	0.31	0.10	8
S	0.10	0.01	0.61	0.20	9	0.40	0.13	0.75	0.26	4	1.58	0.01	5.14	2.06	8
L.O.I.	1.13	0.33	2.59	0.65	9	1.87	1.38	2.21	0.41	4	2.39	0.69	5.27	1.54	8
Total	99.6					100.2					99.4				
Rb	6	2	17	5	9	5	1	7	3	4	19	3	33	10	8
Ba	331	100	1,200	384	8	370	100	800	376	3	1,545	520	3,900	1,601	4
Sr	203	107	316	76	8	69	32	108	34	4	149	33	219	70	8
Sc	38	32	47	5	7	115	30	280	143	3	45	31	67	16	4
V	283	250	325	30	7	280	260	290	17	3	278	230	330	41	4
Cr	210	150	260	44	7	285	240	330	64	2	245	180	290	54	4
Co	149	40	656	221	9	222	33	568	248	4	43	30	51	9	4
Ni	317	61	563	183	9	297	142	515	181	4	330	176	506	105	8
Cu	81	50	145	34	9	201	94	345	122	4	70	53	85	12	8
Zn	164	122	222	37	7	282	259	305	33	2	488	136	1,800	587	8
La	7.9	3.5	16.0	3.9	7	5.2	3.4	7.3	2	3	7.3	6.0	10.0	1.8	4
Ce	22	12	36	8	7	15	11	22	6	3	20	15	29	6	4
Sm	4.8	3.3	7.2	1.3	7	3.4	2.6	4	0.7	3	4.3	3.5	6.0	1.1	4
Eu	1.8	1.3	2.1	0.3	7	1.3	1.1	1.4	0.2	3	1.3	1.2	1.4	0.1	4
Tb															
Dy	6.1	4.6	9.3	1.6	7	4.5	3.4	5.2	1.0	3	6.5	5.6	8.5	1.4	4
Yb	4.0	2.8	5.9	1.0	7	3.0	2.7	3.1	0.2	3	3.6	2.5	5.8	1.5	4
Lu	0.58	0.4	0.85	0.17	6	0.37	0.3	0.48	0.1	3	0.54	0.37	0.79	0.18	4
Y	38	28	55	8	9	28	24	33	4	4	36	29	47	6	8
Zr	138	74	255	51	9	98	79	121	18	4	135	96	194	36	8
Nb	9	6	15	3	9	9	7	10	1	4	10	4	14	3	8
Hf	3.6	2.5	5.9	1.2	7	2.4	2.3	2.5	0.1	2	3.3	2.5	4.9	1.1	4
Rb/Sr	0.029	0.009	0.065	0.017	9	0.06	0.031	0.082	0.021	4	0.192	0.016	0.667	0.203	8
Nb/Y	0.25	0.20	0.32	0.04	9	0.32	0.27	0.37	0.05	4	0.27	0.14	0.38	0.08	8
Zr/Y	3.5	2.6	4.6	0.6	9	3.5	2.9	3.8	0.4	4	3.8	3.1	4.6	0.5	8
Zr/Hf	41	38	48	3	7	47	45	48	2	2	41	40	42	1	4
Zr/TiO_2	0.0073	0.0061	0.0113	0.0016	9	0.0051	0.0039	0.0059	0.0009	4	0.0069	0.0056	0.0104	0.0015	8
Zr/P_2O_5	0.057	0.046	0.079	0.011	9	0.045	0.036	0.057	0.009	4	0.056	0.049	0.069	0.006	8
$[La/Yb]_N$	1.3	0.8	1.8	0.4	7	1.2	0.7	1.6	0.5	3	1.4	1.1	1.7	0.3	4

	KFS-B					KFS-M					KFS-M at Stone Hill mine				
	Mean	Min	Max	1σ	n	Mean	Min	Max	1σ	n	Mean	Min	Max	1σ	n
SiO_2	48.6	42.8	53.9	3.67	7	44.0	42.4	46.1	1.93	3	58.3	51.7	63.9	4.53	4
TiO_2	2.04	1.82	2.33	0.18	7	2.36	1.94	3.11	0.65	3	1.53	1.05	2.13	0.39	4
Al_2O_3	15.4	11.9	22.3	3.61	7	18.2	15.5	22.1	3.48	3	15.9	15.3	16.7	0.50	4
FeOt	16.1	11.4	18.4	2.88	7	16.3	13.7	18.5	2.45	3	13.1	10.9	16.1	1.73	4
MnO	0.30	0.11	0.56	0.17	7	0.03	0.01	0.05	0.02	3	0.48	0.05	0.99	0.41	4
MgO	4.05	1.10	5.80	1.49	7	1.37	0.91	2.24	0.76	3	4.18	1.46	7.47	2.38	4
CaO	2.76	0.70	9.20	2.96	7	2.00	1.11	2.74	0.83	3	2.92	2.35	3.61	0.52	4
Na_2O	2.91	1.50	4.67	1.25	7	2.28	1.66	3.29	0.88	3	2.45	1.25	4.09	1.05	4
K_2O	1.98	0.74	4.03	1.22	7	4.27	2.34	5.42	1.68	3	0.90	0.50	1.72	0.61	4
P_2O_5	0.25	0.19	0.32	0.05	7	0.30	0.20	0.44	0.13	3	0.24	0.19	0.28	0.04	4
S	4.96	2.10	8.17	2.17	7	6.44	5.44	8.03	1.39	3	—	—	—	—	—
L.O.I.	3.14	1.17	4.83	1.14	7	5.89	4.32	8.15	2.00	3	4.71	3.09	7.51	1.67	4
Total	99.9					100.2					100.1				
Rb	24	9	47	13	7	50	29	67	19	3	4	3	4	0.5	2
Ba	4,817	800	7,100	2,396	6	3,200	3,000	3,400	283	2	448	26	827	379	4
Sr	69	39	163	44	7	73	61	84	12	3	81	22	155	59	4
Se	41	35	48	6	6	56	39	73	24	2	36	20	53	12	4
V	307	270	380	41	6	423	300	545	173	2	—				4
Cr	247	150	370	82	6	305	230	380	106	2	177	99	221	47	4
Co	79	15	284	93	7	46	46	46		1	28	21	33	4	4
Ni	238	103	349	89	7	298	220	347	68	3	162	49	297	88	4
Cu	208	67	810	267	7	128	80	171	46	3	59	29	86	26	
Zn	2,714	168	7,731	3,016	6	1,724	208	4,203	2,165	3	1,519	120	4,670	1,847	
La	7.7	4.7	10	2.1	6	8.3	8.0	8.6	0.4	2	9.4	1.2	25.7	9.9	4
Ce	22	14	31	7	6	27	26	28	1	2	25	4	66	25	4
Sm	4.6	3.5	6.1	1.0	6	7.2	7.2	7.2		1	4.2	1.8	8.8	2.8	4
Eu	1.3	0.6	2.1	0.5	6	2.0	1.9	2.0	0.1	2	1.4	0.7	2.5	0.7	4
Tb											0.8	0.4	1.6	0.5	4
Dy	5.9	3.4	7.9	1.6	6	8.8	7.5	10.0	1.8	2					
Yb	3.9	2.8	6.3	1.3	6	5.2	4.7	5.7	0.7	2	3.3	2.1	5.9	1.5	4
Lu	0.62	0.46	0.88	0.17	6	0.76	0.62	0.89	0.19	2	0.5	0.3	0.9	0.48	4
Y	36	28	46	6	7	40	29	48	10	3	30	23	49	11	4
Zr	153	109	209	41	7	171	118	212	48	3	162	86	264	73	4
Nb	10	7	14	2	7	10	8	12	2	3	14	7	30	9	4
Hf	3.7	2.8	5.2	1.0	6	4.8	4.4	5.2	0.6	2	3.9	1.6	9.0	3.0	4
Rb/Sr	0.404	0.118	0.659	0.208	7	0.709	0.387	1.098	0.360	3	0.030	0.020	0.025	0.005	2
Nb/Y	0.29	0.24	0.36	0.04	7	0.27	0.23	0.29	0.03	3	0.42	0.30	0.61	0.13	4
Zr/Y	4.2	3.2	4.8	0.5	7	4.3	4.1	4.4	0.2	3	5.3	3.7	7.6	1.5	4
Zr/Hf	40	34	53	7	6	42	41	42	1	2	52	29	62	14	4
Zr/TiO_2	0.0069	0.0051	0.0088	0.0015	7	0.0065	0.0055	0.0079	0.0012	3	0.0102	0.0073	0.0129	0.0020	4
Zr/P_2O_5	0.055	0.043	0.065	0.007	7	0.054	0.044	0.064	0.010	3	0.068	0.032	0.094	0.027	4
$[La/Yb]_N$	1.3	1	1.8	0.3	6	1.1	1.0	1.2	0.1	2	0.25	0.05	0.53	0.2	4

Notes: Major elements in wt %; trace elements in ppm; total = ΣXRF + S + L.O.I. − O ≡ S; FeO_{total} = total iron as FeO

Abbreviations: KA = Ketchepedrakee Amphibolite, KGS = Ketchepedrakee garnet schist, KFS-H = hornblende-rich Ketchepedrakee felsic schist, KFS-B = biotite-rich Ketchepedrakee felsic schist, KFS-M = muscovite-rich Ketchepedrakee felsic schist, *n* = number of analyses, $[La/Yb]_N$ = chondrite-normalized ratio

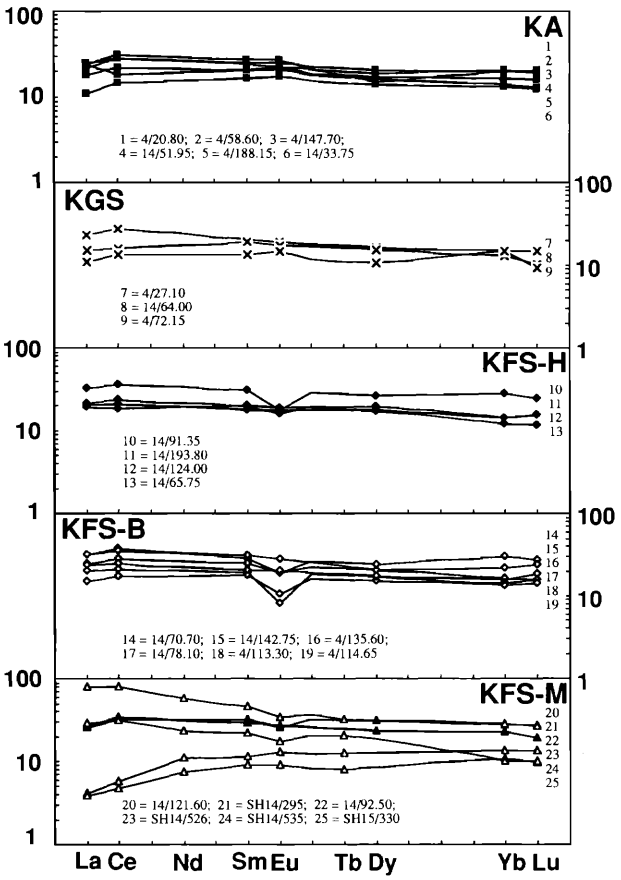

FIG. 7. Chondrite-normalized rare earth element distribution patterns for principal lithologies at the First Wood's prospect. A. Ketchepedrakee Amphibolite (KA). B. Ketchepedrakee garnet schist (KGS). C. Hornblende-rich Ketchepedrakee felsic schist (KFS-H) and biotite-rich Ketchepedrakee felsic schist (KFS-B). D. Muscovite-rich Ketchepedrakee felsic schist (KFS-M). Normalizing values after Taylor and Gorton (1977). The similar, relatively flat patterns (except for variable Eu anomalies) for all rock types are consistent with a common mafic igneous protolith (precursor of the amphibolite). Patterns 21, 23, 24, and 25 are from the Stone Hill mine.

pretations are probably incorrect. The lithological, petrographic, and geochemical evidence for such an interpretation are discussed below.

Lithologic and petrographic evidence: The mineralized Ketchepedrakee felsic schist is highly localized and spatially associated with the amphibolite (Figs. 1-3). Topographic variations, selective erosion, and deformation may also have influenced the distribution of the felsic schist, but if real, its limited lateral extent is incompatible with a sedimentary protolith which would be expected to be laterally more extensive than has been observed. The close interlayering of the felsic schist and the amphibolite in some areas is incompatible with a felsic volcanic protolith, since felsic lavas are very viscous and are not normally interlayered on such a small scale. Felsic tuffs would also be expected to be laterally more extensive than have been observed, although even if transported and deposited in topographic lows in a subaqueous environment, they should contain a significant sedimentary component in such a sediment-dominated sequence as the Ashland Supergroup (Neathery, 1975; Tull, 1978). The abundant isolated pods or lenses (2-5 cm thick) of amphibolite within hornblende- and biotite-rich felsic schist are very significant; many are too large to represent sedimentary fragments and others are too small to represent intercalated flows or tuffs; structural analysis indicates that they do not represent infolded layers (Niu, 1988).

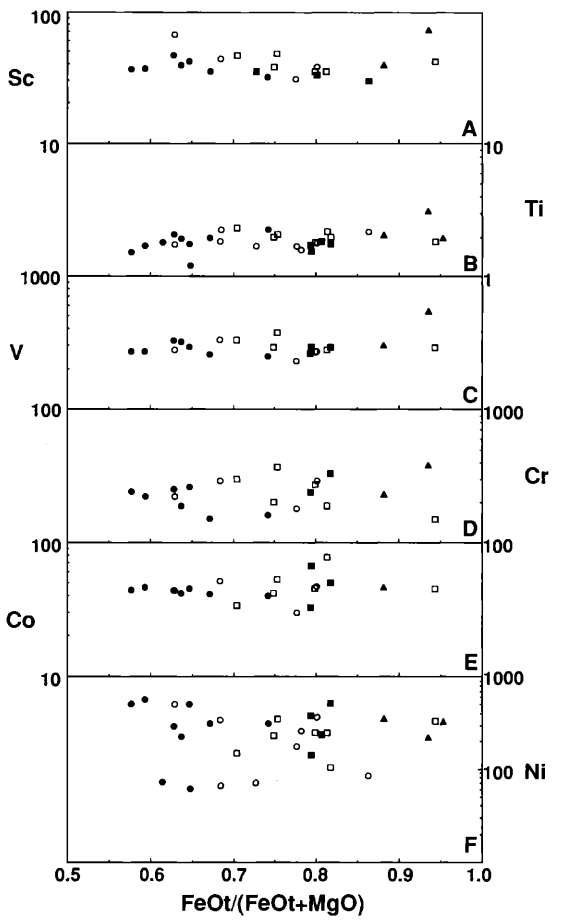

FIG. 8. FeO°/(FeO° + MgO) variation diagrams for compatible elements in the Ketchepedrakee Amphibolite (KA) the garnet schist (KGA), and the hornblende (KFS-H)-, biotite (KFS-B)-, and muscovite (KFS-M)-rich felsic schist at the First Wood's prospect. A. Sc. B. Ti. C. V. D. Cr. E. Ni. F. Co. The constant and uniformly high abundances of compatible elements in all rock types are consistent with a mafic igneous protolith. Only Ni, which may be chalcophile under conditions of high f_{S_2}, appears to have been significantly mobile. Symbols: filled circles = KA, filled squares = KGS, open circles = KFS-H, open squares = KFS-B, filled triangles = KFS-M.

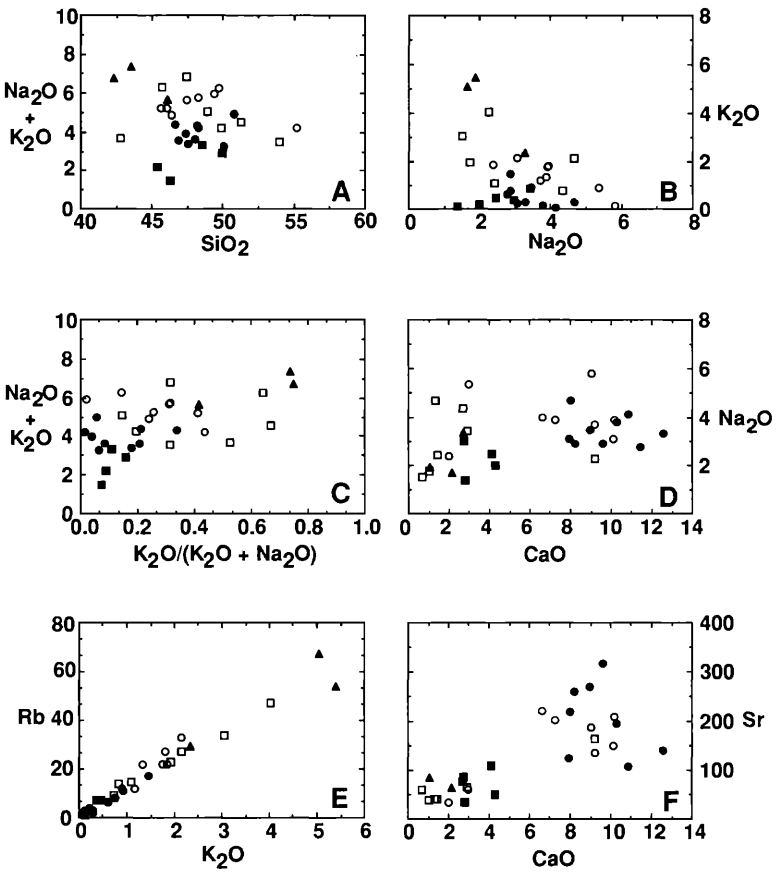

FIG. 9. Variation diagrams for SiO_2 and calc-alkaline elements in the Ketchepedrakee Amphibolite (KA), the garnet schist (KGA), and the hornblende (KFS-H)-, biotite (KFS-B)-, and muscovite (KFS-M)-rich felsic schist at the First Wood's prospect. A. $Na_2O + K_2O$ vs. SiO_2. B. K_2O vs. Na_2O. C. $Na_2O + K_2O$ vs. $K_2O/(Na_2O + K_2O)$. D. Na_2O vs. CaO. E. Rb vs. K_2O. F. Sr vs. CaO. The scatter of data points reflects mobility of these elements during hydrothermal alteration, metamorphism, and retrogression. The correlation of Rb and K_2O indicates that they did not decouple during alteration. Sr and CaO exhibit a similar but more disperse relationship, reflecting decoupling during retrogressive carbonation. Symbols as in Figure 8.

The complete lithological and mineralogical gradations from the amphibolite to the garnet schist to the felsic schist are also incompatible with a felsic volcanic protolith for felsic schist. The presence of gradational contacts between amphibolite and felsic schist on both sides of felsic schist units suggests that the felsic schist is not a sediment developed on top of the amphibolite. All major lithologies contain abundant Ti phases: ilmenite in the amphibolite, rutile or sphene in the garnet and felsic and schists. Basalts contain ubiquitous iron-titanium oxides, so the ilmenite in the amphibolite probably formed from igneous titanomagnetite during prograde metamorphism. Although ilmenite and rutile may be hydrodynamically concentrated in sediments, the distribution of Ti-rich phases in the felsic schist is too uniform to represent placer accumulation. The distribution of abundant rutile (or sphene) along the S_1 foliation in two schists is identical to the distribution of abundant ilmenite in the amphibolite and the presence of oriented inclusions of rutile in garnet, biotite, and staurolite in felsic schist indicates that hydrothermal alteration predated prograde metamorphism. The sphene in some felsic schist evidently results from retrograde alteration of rutile in carbonate-rich domains. Both the garnet and felsic schists are pervasively mineralized with sulfides, whereas no sulfides have been recognized in the amphibolite. The presence of ilmenite in the amphibolite and rutile-pyrrhotite in garnet and felsic schists suggests that they are related to the amphibolite by mineralization-associated hydrothermal alteration.

The presence of abundant Ti phases in all rock types indicates that Ti was relatively immobile during hydrothermal alteration and that the relative stability of Ti phases was determined by variations in f_{O_2},

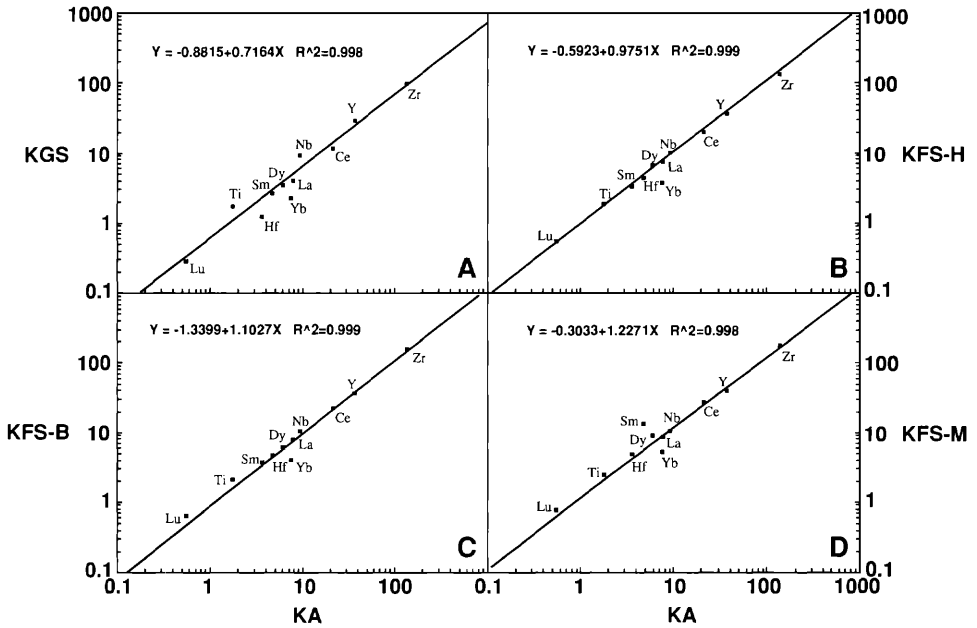

FIG. 10. Regressions of immobile elements in principal lithologies at the First Wood's prospect with respect to those of average Ketchepedrakee Amphibolite (KA). A. Ketchepedrakee garnet schist (KGS). B. Hornblende-rich Ketchepedrakee felsic schist (KFS-H). C. Biotite-rich Ketchepedrakee felsic schist (KFS-B). D. Muscovite-rich Ketchepedrakee felsic schist (KFS-M). The high correlation coefficients indicate a common protolith, the precursor of the amphibolite; deviations of intercepts from zero are within analytical errors; slope deviations from unity reflect concentration-dilution by mobile components and/or volume changes.

f_{CO_2}, and f_{S_2} during alteration and retrograde metamorphism. The rutile and sphene in the garnet and felsic schists are interpreted to have formed by sulfidation of primary ilmenomagnetite during hydrothermal alteration of the precursor to the amphibolite and by retrograde carbonation of rutile, respectively:

$$\underset{\text{ilmenomagnetite}}{Fe(FeTi)_2O_4} + 2H_2S \rightarrow \underset{\text{2 pyrrhotite}}{2FeS} + \underset{\text{rutile}}{TiO_2} + 2H_2O \quad (1)$$

and

$$\underset{\text{rutile}}{TiO_2} + \underset{\text{quartz}}{SiO_2} + \underset{\text{calcite}}{CaCO_3} \rightarrow \underset{\text{sphene}}{CaTiSiO_5} + CO_2. \quad (2)$$

Geochemical evidence: Geochemical comparisons of garnet and felsic schists with the amphibolite demonstrate that although these rock types exhibit different mobile element geochemistries, they are virtually identical in their less mobile element geochemistries, suggesting that they are genetically related. The geochemical similarities can be summarized as follows:

1. The amphibolite, garnet schist, and felsic schist all exhibit relatively consistent and high abundances of compatible elements such as Sc, Ti, V, Cr, Co, and Ni (Fig. 8A-F) that should be greater in mafic volcanic rocks and less in felsic volcanic or sedimentary rocks. The high Ti content of the three lithologies (1.1–3.1%) is similar to that of common mafic igneous rocks but is much greater than that of felsic igneous rocks (max 0.68%: Nockold, 1954) and sedimentary rocks (max 1.13% for shale: Chester and Johnson, 1971). The relatively constant abundances of compatible elements at different Mg/Fe ratios and amounts of sulfur are not consistent with igneous fractionation, because they should be depleted during fractionation, or with addition during sulfidation. Ni exhibits more scatter, probably owing to remobilization during alteration (it is more chalcophile than the other elements).

2. The REE distribution patterns of the felsic schist are very similar to those of the amphibolite and the garnet schist (Fig. 7A-E) and are comparable to the slightly light REE-depleted to light REE-enriched patterns of most tholeiitic basaltic rocks (Saunders, 1984). They are distinct from the light REE-enriched patterns of most, but not all, felsic volcanic rocks (e.g., Lesher et al., 1986a). If the felsic schists were formed by fractionation of the basalts (precursor of the amphibolite), then the felsic schists should be enriched in light REE and other incompatible elements. REE patterns of sediments are very variable, depending on the composition of the source material and the

weathering process, but most are more light REE enriched than the felsic schist, including the North American shale composite and Holocene river sands (Taylor and McLennan, 1985) and Wedowee Group metasediments of the adjacent Tallapoosa block (C. M. Lesher, unpub. data).

3. Elements such as Y, Zr, Nb, Hf, Ti, and REE in the garnet and felsic schists exhibit relatively constant ratios that are virtually identical to those in the amphibolite (Table 3). Regressions of the abundances of these elements in the garnet schist and the hornblende-, biotite-, and muscovite-rich felsic schist with respect to those in the amphibolite (Fig. 10A–D) yield correlation coefficients (r^2) greater than 0.995 and regression lines that pass through the origin (within analytical and statistical errors).

The above geochemical data strongly suggest that the felsic schist is neither a metasediment nor a felsic metavolcanic rock, but that it and the garnet schist are altered equivalents of the amphibolite. That is, all three major lithologies have been derived from the same protolith, the precursor to the amphibolite. This is also consistent with the lack of significant Pb in these deposits (galena is absent); as a compatible element in felsic igneous systems, felsic volcanic rocks are enriched in Pb and mafic igneous rocks are depleted in Pb. The constant interelement ratios of the high field strength elements suggests that they were relatively immobile during alteration. The variations in slopes of the regression lines between different rock types and the deviations from unity are interpreted to represent concentration and dilution by mobile elements during mineralization-related hydrothermal alteration and, to a lesser extent, retrograde alteration.

The above interpretation is further supported by factor analysis (Niu, 1988). Q mode factor analysis indicates that all three lithologies are essentially autocorrelated, implying they have a common protolith. R mode factor analysis suggests that the transformation of amphibolite to garnet schist and felsic schist results from mineralization-associated hydrothermal alteration.

Mass balance calculations

Assuming that the garnet and felsic schists are derived from the precursor of the amphibolite by premetamorphic hydrothermal alteration, the geochemical changes that accompanied this alteration can be evaluated through mass balance calculations (Gresens, 1967; Grant, 1986). Such calculations are based on the assumption that some elements are immobile during alteration and that these elements can be used to constrain mass and/or volume changes during alteration.

Because the alteration in the Stone Hill district is shown to have occurred prior to penetrative deformation and metamorphism, it is not possible to distinguish volume changes associated with alteration. As such, the emphasis of the calculations has been to determine mass changes in the altered rocks. Isocon diagrams were constructed using least mobile, high field strength elements with constant interelement ratios (Fig. 10A-D), the slopes of regression lines (isocons) were calculated and normalized to unity (zero volume change), and the resulting factors were used to normalize the abundances of all analyzed elements to zero volume change. The net enrichments and depletions of all analyzed elements in the garnet and felsic schists are plotted relative to those in least altered amphibolite in Figure 11A-D.

The garnet schist is depleted in K, Na, Sr, Ca, Eu, REE, and Hf and enriched in Al, first-period transition metals (Mn, Fe, Co, Ni, Cu, Zn, Sc, Ti), and S relative to the amphibolite (Fig. 11A). This alteration signature is very similar to that observed in less metamorphosed chloritized mafic volcanic rocks in the Noranda mining district, Quebec (Lesher et al., 1986b).

The hornblende-rich felsic schist is depleted in Sr, Ca, Mg, Ni, and Eu and enriched in Rb, K, Ba, Mn, Cu, Zn, and S relative to the amphibolite (Fig. 11B). The biotite-rich felsic schist is depleted in Si, Al, Na, Sr, Ca, Mg, Co, Ni, and Eu and enriched in Rb, K, Ba, Mn, Cu, Zn, and S (Fig. 11C). The muscovite-rich felsic schist is depleted in Si, Na, Sr, Ca, Mg, Mn, Co, and Eu and enriched in Rb, K, Ba, Zn, and S (Fig. 11D). The relative degrees of enrichment or depletion increase systematically from hornblende- to biotite- to muscovite-rich felsic schist. This is consistent with the gradational mineralogical relationships between amphibolite and felsic schist. The alteration signature of the felsic schist is very similar to that observed in less metamorphosed sericitized mafic volcanic rocks in the Noranda mining district, Quebec (Lesher et al., 1986b).

The felsic schist is considerably more enriched in sulfur than in Fe, Zn, or Cu (ca. 40× vs. 1.3× expected from sulfide stoichiometry), indicating that sulfur was more abundant than metals in the hydrothermal fluid and that metal availability rather than sulfur availability was the limiting control on the degree of mineralization.

District-scale geochemical variations in the Ketchepedrakee felsic schist

Because surface exposure at the Stone Hill mine is limited, the shaft is collapsed, and available drill core is skeletonized, it is not possible to establish macroscopic relationships between the mineralized felsic schists and the associated garnet schist and amphibolite. However, lithologic and petrographic studies of the felsic schist at the Stone Hill mine indicate that it is very similar to that at the First Wood's prospect in terms of gradations in lithology, mineralogy, styles

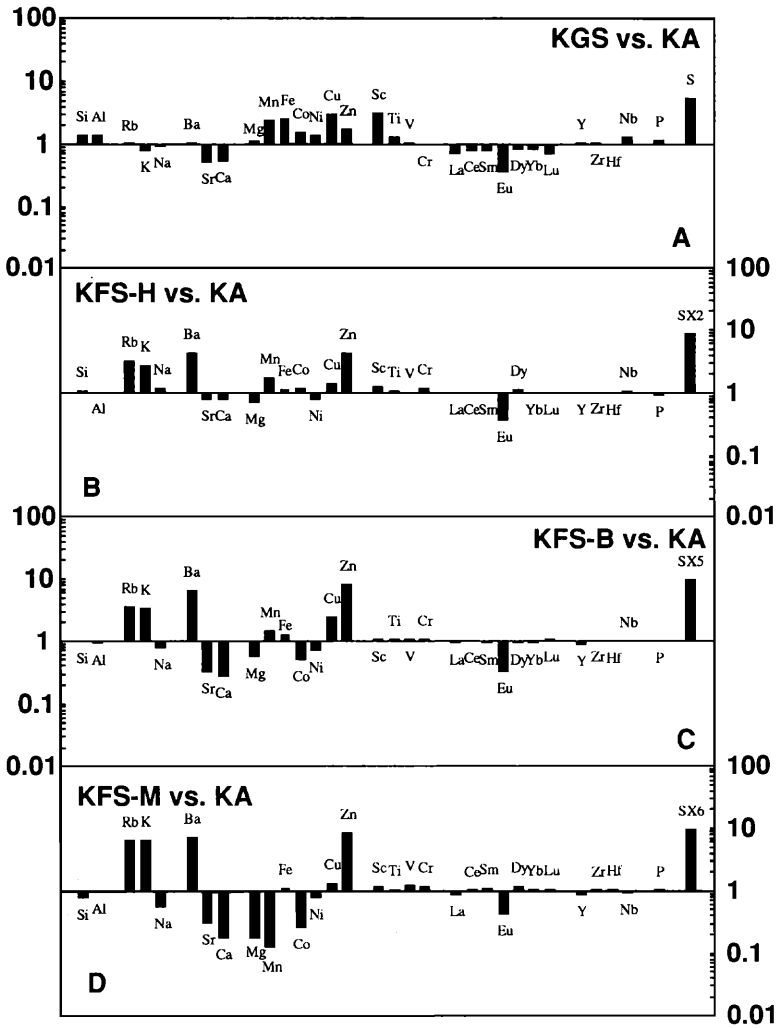

FIG. 11. Absolute mass enrichments or depletions for principal lithologies at the First Wood's prospect with respect to those of average Ketchepedrakee Amphibolite (KA). A. Ketchepedrakee garnet schist (KGS). B. Hornblende-rich Ketchepedrakee felsic schist (KFS-H). C. Biotite-rich Ketchepedrakee felsic schist (KFS-B). D. Muscovite-rich Ketchepedrakee felsic schist (KFS-M). Enrichments or depletions are based on analyzed elemental concentrations, normalized to constant mass of immobile elements using calculated slopes of regression lines in Figure 11 (see explanation in text); values greater than 1 represent enrichment, whereas values less than 1 represent depletion.

of deformation, and distribution of Ti-rich phases. This suggests that the felsic schist at Stone Hill is also not a felsic metavolcanic rock or metasediment. As such, the variability in Sc, Cr, light REE, Y, Zr, and Nb in the felsic schist at the Stone Hill mine (Table 3) may reflect primary igneous variations within the mafic volcanic rocks, or variable degrees of mobility of these elements during alteration. With only four analyses it is difficult to make an unequivocal interpretation, but it is difficult to conceive of a magmatic process that would fractionate light REE from heavy REE in a mafic magma or lava, so the variations in compatible elements and corresponding variations in incompatible elements (light REE, Y, Zr, and Nb) in the Stone Hill samples are interpreted to result from varying degrees of ore-related hydrothermal alteration.

The significantly higher Zr contents in the felsic schist from the Chaotic Zone and Johnson prospects reported by Schafer and Coolen (1986) may therefore represent more extensively altered equivalents of the felsic schist at the First Wood's prospect and Stone Hill mine. Similarly, the variations in Mg, Cr, and Ni in the amphibolite at Stone Hill reported by Whittington (1986) may also be attributable to alteration.

Based on detailed studies of alteration associated with several Canadian massive sulfide deposits,

Campbell et al. (1984) reported that REE, Ti, Y, Zr, and Nb were relatively immobile during slight to moderate degrees of alteration but that all elements may be mobile during extreme alteration associated with large volcanogenic massive sulfide deposits. Their work suggests that the mobility of REE and high field strength elements increases with the size of deposits and with the size of the associated alteration system. The amount of altered rock in the Stone Hill district is greatest around the Chaotic Zone and Johnson prospects (Fig. 1), suggesting that those areas were the loci of greatest fluid flow and hydrothermal alteration.

Tectonic setting and environment of deposition

Interpretation of the Ketchepedrakee Amphibolite as a tholeiitic basalt, the Ketchepedrakee garnet and felsic schists as metamorphosed, hydrothermally altered variants of the amphibolite, and the enclosing graphitic and garnetiferous schists as metamorphosed flysch-type sedimentary rocks suggests that the rocks of the Stone Hill district were deposited in an incipiently rifted basin or along a rifted continental margin rather than in a back-arc basin as proposed by Neathery and Hollister (1984). There is no evidence of felsic volcanic rocks and therefore no evidence for a volcanic arc. The Ketchepedrakee Amphibolite and other amphibolite bodies recognized in the Coosa block are only minor units enclosed within thick sedimentary sequences and there is no indication that they represent oceanic crust. The interpretation that the Stone Hill mine deposit formed in an ocean-floor spreading setting (Whittington, 1986) is similarly invalid.

The Stone Hill deposits are best classified as ensialic massive sulfide deposits (Stephens et al., 1984) associated with a continental margin rather than as Besshi-type deposits associated with a back-arc basin. Volcanic-associated massive sulfide deposits have been divided on the basis of proximity to hydrothermal discharge sites into proximal and distal types (Franklin et al., 1981). The close genetic relationship between mineralization and hydrothermal alteration in the Stone Hill district indicates a proximal volcanic environment.

Genetic model

The preferred model involves clastic sedimentation (Ashland Supergroup), basaltic volcanism (Ketchepedrakee Amphibolite), and hydrothermal activity (Ketchepedrakee garnet schist and felsic schist and associated alteration lithologies) in an incipiently rifted basin. This basin may have been produced in response to the eastern North American continental rifting event during late Precambrian to Early Cambrian, in association with opening of the Iapatus ocean (Hatcher, 1978).

High-angle normal faults required for rifting may have acted as passages through which basaltic volcanism and waning-stage hydrothermal activity were focused. Such hydrothermal activity was responsible for local alteration of the mafic volcanic rocks (precursor of the amphibolite) to produce chloritized (the garnet schist) and sericitized (the felsic schist) equivalents, and transportation and precipitation of ore metals to form the Fe-Cu-Zn sulfide deposits in the Stone Hill district. Fluid conduits would be difficult to recognize in such a polydeformed and metamorphosed area, but the copper-enriched garnet schist lithologies are the best candidates for hydrothermal discharge sites.

The continuous and gradational variations in the abundances of hornblende, quartz, feldspar, biotite, muscovite, garnet, rutile, and sulfides, from the amphibolite through hornblende- and biotite-rich felsic schist to the muscovite-rich felsic schist, and from the amphibolite to the garnet schist, indicate that mineralization occurred during hydrothermal alteration. S_1 foliations defined by Ti phases and pyrrhotite are overgrown by prograde silicate minerals, which indicates that this alteration predated regional prograde metamorphism. Alteration is absent in the interpreted hanging-wall rocks. Hydrothermal alteration and mineralization are therefore interpreted to have occurred at the synvolcanic stage, after emplacement of the precursor of the amphibolite, but prior to deposition of the overlying graphitic sediments of the Poe Bridge Mountain Group. This hydrothermal alteration was not only responsible for the chemical transformation of the amphibolite to the garnet and felsic schists but was also responsible for the sulfide mineralization. The source of the ore constituents is still an unsolved problem in the genesis of most volcanic-associated massive sulfide deposits (Franklin et al., 1981). Factor analysis (Niu, 1988) separates ore-related elements into two multivariate factors, suggesting that ore components have been derived from two different sources. The separation of Fe, Cu, and Zn from S, Ba, K, and Rb, together with the considerable enrichment of sulfur relative to Fe, Cu, and Zn, may indicate that the former components were derived from the mafic volcanic footwall rocks (precursor of the amphibolite), whereas the latter components were derived from the enclosing metasediments (Ashland Supergroup). Isotopic data will be required to test this possibility. This genetic model is consistent with the base metal zonation sequence observed at the First Wood's deposit (Fig. 3), from stratigraphically lowest to highest: Cu in the garnet schist, Zn-(Cu) in the felsic schist, and Fe in iron-formation. By analogy with less deformed deposits in the Canadian Shield (Large, 1978; Franklin et al., 1981) this zonation is interpreted to reflect differences in the solubilities of base metals in the hydro-

thermal system and suggests that the sequence at the First Wood's prospect is overturned (Schafer and Coolen, 1986).

Volcanic-associated massive sulfide deposits form as a result of hydrothermal activity and large deposits require commensurately large hydrothermal systems with high fluid/rock ratios. The apparent limited extent of the mineralization in the Stone Hill district can be attributed to small-scale hydrothermal activity brought about by the relatively low abundance of volcanic rock in the sequence which suggests only incipient rifting and consequently low heat flow. Because volcanic-associated massive sulfide deposits are considered to precipitate from convecting hydrothermal fluids, low heat flow would result in less convection and lower solubility of base metals in the fluid. This is supported by the limited extent of altered rocks in the district (Figs. 1 and 2), consistent with small-scale hydrothermal activity. Therefore, future exploration for similar deposits in this part of the southern Appalachians should be focused in areas with greater quantities of metavolcanic rocks and associated altered lithologies (garnet and felsic schists).

Conclusions

The major conclusions of this study are as follows:

1. Trace element geochemical data obtained in this study confirm previous interpretations that the protolith of the Ketchepedrakee Amphibolite is a tholeiitic basalt.

2. Mineralized felsic schist in the Stone Hill district is neither metasedimentary rock nor metarhyolitic or felsic metapyroclastic rock. It is interpreted to represent a metamorphosed, hydrothermally altered equivalent of the Ketchepedrakee Amphibolite, formed by interaction with sulfur-enriched hydrothermal fluids during the waning stages of basaltic volcanism.

3. The sulfide mineralization in the Stone Hill district resulted from the above hydrothermal alteration. The zonation from Cu (±Zn) in the garnet schist through Zn (±Cu) in the felsic units to Fe in iron-formation is identical to that observed in similar but less deformed massive sulfide deposits.

4. The tectonic setting of ore deposition was most likely a rifted continental margin rather than a back-arc basin or a spreading center. Mafic volcanism was very localized within a thick sedimentary sequence of continental affinity; there is no evidence for the existence of basaltic oceanic crust or felsic volcanism.

5. A proximal volcanogenic model best explains the mineralization in the Stone Hill district. This model involves clastic sedimentation, local basaltic volcanism, and hydrothermal alteration in an incipiently rifted basin. This probably occurred in response to the eastern North American continental rifting event during the late Precambrian to Early Cambrian. Hydrothermal activity during the waning stages of basaltic volcanism was responsible for alteration of basalt (precursor of Ketchepedrakee Amphibolite) to produce the protoliths of felsic schists and garnet schists, and for the transport and precipitation of ore metals. By analogy with less deformed deposits in the Canadian Shield, the garnet schists (chloritic alteration zones) may represent deformed, metamorphosed hydrothermal discharge sites.

6. Minor geochemical differences between mineralized felsic schists in the Stone Hill district are interpreted to reflect variable degrees of alteration. As the inferred degree of alteration and extent of alteration are greatest at the Chaotic Zone and Johnson prospects, these areas may represent larger hydrothermal systems and should receive priority in further exploration.

Acknowledgments

This paper constitutes part of Y.N.'s masters thesis research at the University of Alabama. We are very grateful to Billiton Exploration U.S.A., Inc., for granting access to their lease in the Stone Hill district and providing copies of maps, drill logs, and unpublished company reports; Billiton Exploration U.S.A., Inc., and Tennessee Chemical Corporation for donating diamond drill cores to the University; Marc Coolen for discussions on the geology of the area; Bill Young for his hospitality during the field work; Geoff Gleason and Louise Corriveau for neutron activation analyses; and Gail Davis for sulfur analyses. Constructive comments by *Economic Geology* reviewers are much appreciated. Financial support was provided by the University of Alabama School of Mines and Energy Development (grant 2-29088 to C.M.L.).

August 1, 1990; February 20, 1991

REFERENCES

Brimhall, G. H., and Crerar, D. A., 1987, Ore fluids: Magmatic to supergene: Rev. Mineralogy, v. 17, p. 236–322.

Campbell, I. H., Lesher, C. M., Coad, P., Franklin, J. M., Gorton, M. P., and Thurston, P. C., 1984, Rare-earth element mobility in alteration pipes below massive sulfide deposits: Chem. Geology, v. 45, p. 181–202.

Carmichael, I. S. E., Turner, F. J., and Verhoogen, J., 1972, Igneous petrology: New York, McGraw-Hill, 793 p.

Carpenter, R. H., 1974, Pyrrhotite isograd in southern Tennessee and southwestern North Carolina: Geol. Soc. America Bull., v. 85, p. 451–456.

Chester, R., and Johnson, L. R., 1971, Trace element geochemistry of North Atlantic aeolian: Nature, v. 231, p. 176.

Espenshade, G. H., 1963, Geology of some copper deposits in North Carolina, Virginia, and Alabama: U.S. Geol. Survey Bull. 1142-I, 51 p.

Franklin, J. M., Lydon, J. W., and Sangster, D. F., 1981, Volcanic-associated massive sulfide deposits: ECON. GEOL. 75TH ANNIV. VOL., p. 485–627.

Grant, J. A., 1986, The isocon diagram—a simple solution to Gresens' equation for metasomatic alteration: ECON. GEOL., v. 81, p. 1976–1982.

Gresens, R. L., 1967, Composition-volume relationships of metasomatism: Chem. Geology, v. 2, p. 47–65.

Hatcher, R. D., Jr., 1978, Tectonics of the west Piedmont and Blue Ridge, southern Appalachian: Am. Jour. Sci., v. 278, p. 276–304.

Holland, J. G., and Winchester, J. A., 1983, The use of geochemistry in solving problems in highly deformed metamorphic complexes, *in* Augustithis, S. S., ed., The significance of trace elements in solving petrogenetic problems and controversies: Athens, Theophrastus, p. 384–405.

Large, R. R., 1978, Chemical evolution and zonation of massive sulfide deposits in volcanic terrains: ECON. GEOL., v. 72, p. 549–572.

Lesher, C. M., Goodwin, A. M., Campbell, I. H., and Gorton, M. P., 1986a, Trace-element geochemistry of ore-associated and barren, felsic metavolcanic rocks in the Superior province, Canada: Canadian Jour. Earth Sci., v. 23, p. 222–237.

Lesher, C. M., Gibson, H. L., and Campbell, I. H., 1986b, Composition-volume changes during hydrothermal alteration of andesite at Buttercup Hill, Noranda district, Quebec: Geochim. et Cosmochim. Acta, v. 50, p. 2693–2705.

Neathery, T. L., 1967, Paragenesis of the Turkey Heaven Mountain kyanite deposits, Cleburne County, Alabama: Alabama Geol. Survey Circ. 41, 56 p.

—— 1975, Rock units in the high-rank belt of the northern Piedmont, Alabama: Alabama Geol. Soc., 13th Ann. Field Trip Guidebook, p. 9–47.

Neathery, T. L., and Hollister, V. F., 1984, Volcanogenic sulfide deposits in the southernmost Appalachians: ECON. GEOL., v. 79, p. 1540–1560.

Niu, Y., 1988, Hydrothermal alteration of mafic metavolcanic rocks and genesis of Fe-Zn-Cu sulfide deposits, Stone Hill district, northern Piedmont, Alabama: Unpub. M.Sc. thesis, Univ. Alabama, 116 p.

Nockold, S. R., 1954, Average chemical composition of some igneous rocks: Geol. Soc. America Bull., v. 65, p. 1007–1032.

Pallister, H. D., and Thoenen, 1948, Stone Hill copper mine, Cleburne and Randolph Counties, Alabama: U.S. Bur. Mines, Rept. Inv. 4221, 29 p.

Pearce, J. A., and Cann, J. R., 1973, Tectonic setting of basic volcanic rocks determined using trace element analysis: Earth Planet. Sci. Letters, v. 19, p. 290–300.

Rösler, H. J., and Beuge, P., 1983, Geochemistry of trace elements during regional metamorphism, *in* Augustithis, S. S., ed., The significance of trace elements in solving petrogenetic problems and controversies: Athens, Theophrastus, p. 406–430.

Saunders, A. D., 1984, The rare earth element characteristics of igneous rocks from the ocean basins, *in* Fyfe, W. S., ed., Rare earth element geochemistry: New York, Elsevier, p. 205–236.

Schafer, R. W., and Coolen, J. M., 1986, Sulfide mineralization along the southern flank of Turkey Heaven Mountain, Cleburne County, Alabama: Univ. Tennessee Dept. Geol. Sci., Studies in Geology, v. 16, p. 22–49.

Stephens, M. B., Swinden, H. S., and Slack, J. F., 1984, Correlation of massive sulfide deposits in the Appalachian-Caledonian orogen on the basis of paleotectonic setting: ECON. GEOL., v. 79, p. 1442–1478.

Stow, S. H., Neilson, M. J., and Neathery, T. L., 1984, Petrography, geochemistry and tectonic significance of the amphibolites in the Alabama Piedmont: Am. Jour. Sci., v. 284, p. 414–436.

Stow, S. H., Whittington, D., and Tull, J. F., 1985, The Pyriton and Stone Hill massive sulfide deposits of the Alabama Piedmont: A comparison [abs.]: Geol. Soc. America Abstracts with Programs, v. 17, p. 138.

Taylor, S. R., and Gorton, M. P., 1977, Geochemical application of spark source mass spectrography—III. Element sensitivity, precision and accuracy: Geochim. et Cosmochim. Acta, v. 41, p. 1357–1380.

Taylor, S. R., and McLennan, S. M., 1985, The composition of the continental crust: Its composition and evolution: Surrey, U.K., Blackwell Sci. Pub., 312 p.

Tull, J. F., 1978, The structural development of the Alabama Piedmont northwest of the Brevard zone: Am. Jour. Sci., v. 278, p. 442–460.

Whittington, D., 1982, Geology of the Stone Hill massive sulfide copper mine, Cleburne and Randolph Counties, Alabama: Unpub. M.Sc. thesis, Univ. Alabama, 143 p.

—— 1986, Stratigraphic and chemical prospecting criteria for base metal sulfide deposits in polydeformed high-grade metamorphic settings: Univ. Tennessee Dept. Geol. Sci., Studies in Geology, v. 16, p. 50–66.